Transient Thermo-Reflectance Measurements of the Thermal Conductivity and Interface Resistance of Metallized Natural and Isotopically-Pure Silicon

Pavel L. Komarov, Mihai G. Burzo, Gunhan Kaytaz, and Peter E. Raad
Submicron Electro-Thermal Sciences Laboratory,
Department of Mechanical Engineering
Southern Methodist University
Dallas, TX 75275-0337, U.S.A.
E-mail: praad@mail.smu.edu

Abstract

The transient thermoreflectance method has been used to measure the thermal conductivity of natural silicon and isotopically-pure silicon-28 layers that are epitaxially grown on natural silicon substrates. The measurements were performed at room temperature for both a low level (1×10^{16}) and a higher level (2×10^{19}) of Boron doping of the epitaxial layers. The results indicate a gain of approximately 55% in the thermal conductivity of Si28 as compared to that of natural Si, at both low and higher levels of doping, and a decrease of approximately 19% in the thermal conductivity for both types of silicon due to the higher level of doping.

1. Introduction

The miniaturization and performance requirements of modern high power electronic devices have forced the development of special materials [1]. Significant gains in the performance and reliability of electronic and telecommunication devices can be achieved by maintaining their active areas at low temperature levels. A direct approach to achieving lower temperatures in these areas is to utilize materials whose thermal conductivity is high. However, the choice of materials is naturally limited to those normally used in semiconductor devices. One promising approach is that of the use of isotopically-pure semiconductor materials, whose thermal conductivity is suspected to exceed that of their natural counterparts. As reported by Capinski et al. [2], the isotopically-pure silicon, germanium, and diamond exhibit gains in thermal conductivity at room temperature of up to 60%, 30%, and 50%, respectively. A later investigation that made use of a steady-state heat-flow experimental technique [3] revealed the same result of 60% increase in the thermal conductivity for isotopically-pure Si^{28}.

While exciting, such gains in conductivity are surprising, which may in part explain the hesitancy of the industry in adopting the use of isotopically-pure silicon. Also, the materials that Capinski et al. investigated were intrinsic, which leaves open the question of whether doping would drown out the gains observed for isotopically-pure materials.

Consequently, the objectives of this work are both to confirm the above mentioned gains in thermal conductivity for isotopically-pure Si and to assess the influence of doping concentration (which is expected to have a negative effect on the thermal conductivity).

Thermal conductivity measurements have been carried out by the use of a transient thermoreflectance (TTR) method [4], which is favored among the various experimental techniques [5] used to measure the thermal conductivity of thin-film and multi-layered materials. The main advantages of the TTR method is that it is a non-contact and non-destructive optical approach, both for heating the sample and for probing the temperature variations of its surface [6].

2. Measurements Methodology

The schematic in Fig. 1 depicts the square heating and round probing spots produced by the TTR system in the SMU Submicron Electro-Thermal Sciences (SETS) Laboratory (http://www.engr.smu.edu/setsl). The existing

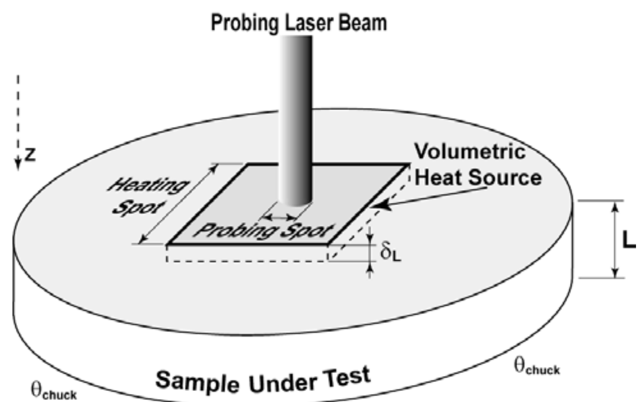

Fig. 1 Schematic of the heating and probing spot positioning on the sample under test

experimental TTR system used is depicted schematically in Fig. 2. The heating source in the measurement apparatus is an Nd:YAG pulsed laser with 532 nm wavelength and up to 0.1 mJ pulse energy. The heating spot of the YAG was characterized by CCD imaging and fast photodiode detection, and was found to have good spatial uniformity and a Gaussian temporal distribution, namely:

$$I(t) = \frac{2F}{\tau\sqrt{\pi}} e^{-4\left(\frac{t-t_0}{\tau}\right)^2} \qquad (1)$$

Here, F is the fluence of laser irradiation, $t_0 = 9.6$ ns is the time at which the intensity reaches its maximum value, and $\tau = 8.6$ ns is the "duration of the laser pulse" (defined as the full-width of the pulse at $1/e$ height). The probing light source is a linearly polarized, single mode Ar-Ion CW laser beam with 488 nm wavelength, and is delivered to the assembly by a polarization-preserving fiber optic cable. The beam then is focused by a microscope objective lens on the sample surface in the middle of the heated spot. The probing beam reflects from the heated sample surface, returns by the same path, and is delivered by a fiber optic assembly to the sensitive area of a preamplified silicon PIN photodiode. The intensity of the reflected light depends on the sample surface reflectivity, which is a function of the surface temperature.

Since the scale of the area heated by the pulsed YAG laser (~200 µm) is much larger than that of the probing spot area (~2.5 µm) as well as the heat penetration depth (~3.5 µm), the one-dimensional heat conduction equation represents well the transient thermal process within the sample:

$$\rho\, C_p \left(\frac{\partial T}{\partial t}\right) = \frac{\partial}{\partial z}\left(K \frac{\partial T}{\partial z}\right) + \dot{Q}(z,t) \qquad (2)$$

Here, ρ is the material density, C_p is the heat capacity, K is the material thermal conductivity, and $\dot{Q}$ is the heat source term which is a function of the depth, z, which is measured downwardly from the top surface of the gold, and time, t.

The boundary conditions used are $(\partial T/\partial z) = 0$ at the top surface of the gold layer (i.e., $z = 0$) and $T = T_{chuck}$ at the bottom surface of the substrate, while the initial condition at $t = 0$ is $T = T_{ambient} = T_{chuck}$. The heat equation is solved by a central finite difference approach with a three-point-backward temporal scheme (derived from a general Padé-type formulation in order to take advantage of its second-order accuracy and unconditional stability).

3. Results and Discussion

Four 4-inch, 635 µm-thick, silicon wafers with a 5 µm-thick epitaxial layer of either natural silicon or isotopically-pure Silicon-28 (Table 1) have been studied in this investigation. All samples were covered by a gold layer, which serves the purpose of absorbing the laser power as well as keeping the surface optical properties of the samples identical [7]. The thickness of each of the gold layers listed in Table 1 was carefully measured by the use of a Dektak^{3}ST profiler.

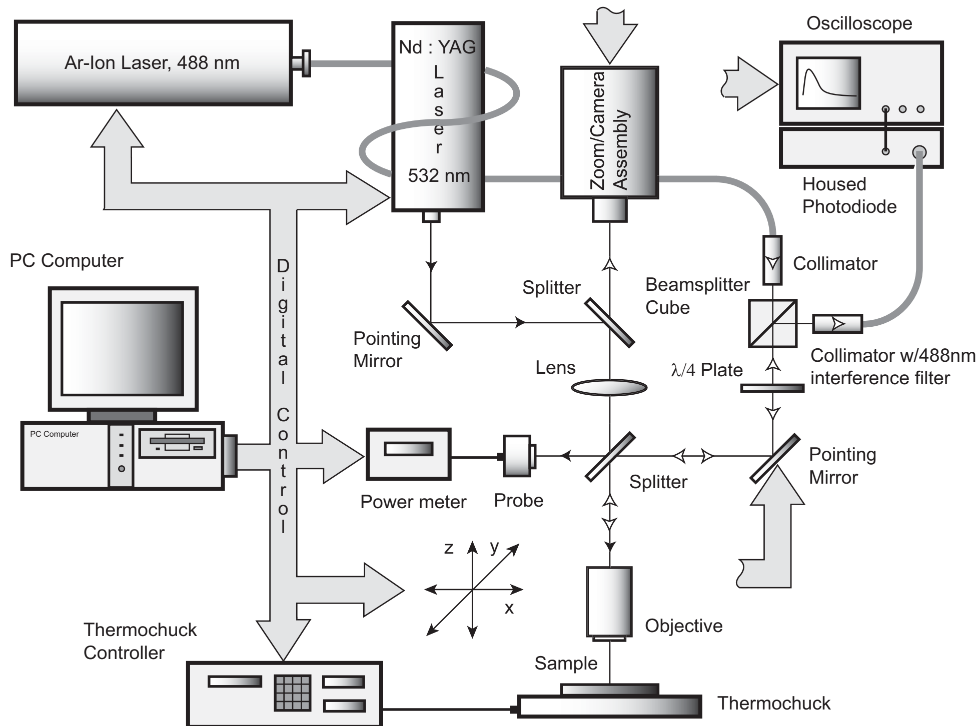

Fig. 2 Schematic of the experimental setup

Table 1 Thermal conductivity and interface resistance measurements for the four samples investigated

Sample No.	Epitaxial Layer		Gold Cover (Å)	K ± σ% (W/m-K)	$R_{th} \times 10^9$ ± σ% (m^2-K/W)
	Type	Doping Level			
1	Nat. Si	1E16	4070 ± 25	148 ± 5.8%	7.4 ± 3.3%
2	Nat. Si	2E19	4010 ± 25	122 ± 6.1%	6.5 ± 14.1%
3	Si^{28}	1E16	5130 ± 25	227 ± 5.7%	5.5 ± 6.8%
4	Si^{28}	2E19	5010 ± 25	190 ± 5.0%	5.5 ± 10.3%

The temperature data points measured for sample 1 are plotted in Fig. 3 along with the curve representing the best fit from the numerical solution of Eq. 2 for that sample. The aim of the fitting procedure is to determine both the thermal conductivity of the epitaxial material and the thermal interface resistance between the epitaxial and gold layers by minimizing the RMS error between the measured response and the numerical solution. If the measurement system were not capable of capturing the thermal physics correctly over the full width of the measurement time window (~250 ns), the raw data points would not have fallen on top of the curve as closely as is evident in Fig. 3. Hence, the excellent agreement between the raw measurement data and the numerical solution is indicative of the quality of the measurement system.

The raw experimental data and corresponding best-fit curves for all four samples are plotted in Fig. 4. The ranges of the time and the normalized temperature axes have been chosen in order to zoom in on the area of interest. The raw temperature responses of samples 1 and 3 appear to fall on top of each other within the uncertainty envelope, as is also the case for samples 2 and 4. The closeness of the plotted responses for the Si and Si^{28} epitaxial materials may lead to the false conclusion that their conductivity values are the same. However, the best-fit matching technique used to deduce the thermal conductivity is influenced by the thickness of the gold layer, which differs by approximately 1000 Å between the natural Si and Si^{28} samples (Table 1). Therefore, seemingly identical normalized response curves lead to measurably different thermal conductivity values.

The observable difference between the responses of the samples with the two levels of doping is entirely attributable to the difference in the thermal conductivity of the epitaxial layer since the gold layer thickness is essentially the same for each pair of Si and Si^{28} samples. The excellent fit between the raw experimental data and numerical results in Fig. 4 indicates both that the experimental measurement system is accurate and that the two-parameter numerical fitting scheme for the thermal conductivity and interface resistance captures all the important physics within the sample under test.

The measured values of the thermal conductivity for the epitaxial material and the thermal interface resistance between the gold and epitaxial layers for the four samples are presented in the two rightmost columns of Table 1, along with the associated percentage uncertainty values. The uncertainty values for each sample are obtained by calculating the standard deviation of ten measurement trials, each consisting of 100 measured temperature responses at the same physical location. The uncertainty

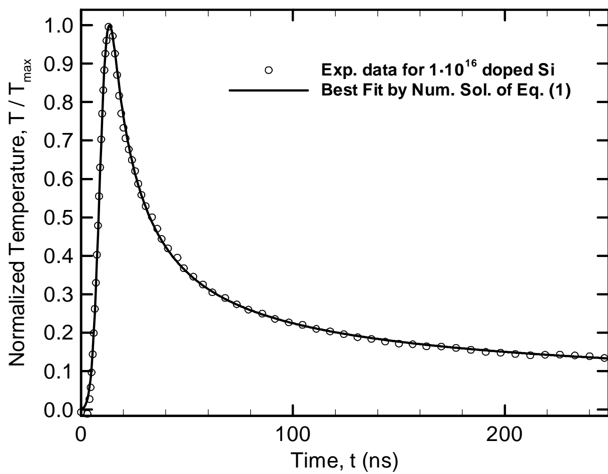

Fig. 3 Normalized temperature response of epitaxially grown natural Si covered by gold (Sample 1)

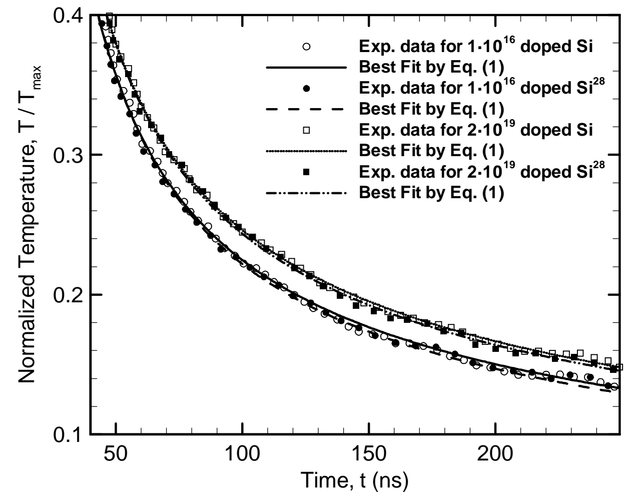

Fig. 4 Comparison of normalized temperature responses of Si and Si28 samples at two different levels of Boron doping

Table 2 Effect of isotopic purity and doping level on thermal conductivity of epitaxial layer

% Change in K (index refers to sample No.)	Photodetector 1		Photodetector 2		Average
	Run 1	Run 2	Run 1	Run 2	
$(K_3 – K_1)/K_1$	53	52	51	60	54
$(K_4 – K_2)/K_2$	56	53	60	56	56
$(K_2 – K_1)/K_1$	–18	–15	–21	–22	–19
$(K_4 – K_3)/K_3$	–16	–15	–16	–23	–18

in the thermal conductivity values is well within the normal acceptable limits of experimental uncertainty.

The measurements presented in Table 1 were made with a fast, preamplified, Si PIN photodiode, referred to hereafter as PD1. In order to validate the reliability of the measurements, the results of another experiment performed with the same photodetector, PD1, as well as two experiments conducted with a similar photodetector, but made by a different manufacturer, and hereafter referred to as PD2, are presented in Table 2. The frequency response of the PD1 is better than that of the PD2 within the range of the transient temperature responses of the samples, but the response of PD1 exhibits increased level of random EMI noise.

The computed value of K = 148 W/m-K for sample 1 (Table 1) falls within the usual range of values reported for natural Si. As observed from examining the last column of Table 2, sample 3 shows a 54% gain in the thermal conductivity at room temperature, as compared with sample 1, indicating that isotopically-pure silicon (Si^{28}) is appreciably more thermally conductive than natural silicon. Comparing the results of the higher doped samples (2 and 4) reveals that the thermal conductivity of sample 4 (Si^{28}) is 56% higher than that of sample 2 (Si). This level of gain is close to the gain observed between the lower doped silicon samples 1 and 3. This consistency provides a level of confidence that Si^{28} is notably more conductive than natural Si, at low, as well as at high levels of doping.

Sample 2 (higher doped Si) shows a 19% decrease in the thermal conductivity as compared to sample 1 (lower doped Si), which is due to the different level of Boron doping in sample 2. Similarly, sample 4 exhibits an 18% drop in the thermal conductivity as compared to sample 3. Since again the only difference between the two samples is the doping level, the drop in conductivity is attributable to the higher doping level of sample 4. The effect of doping on the thermal conductivity of Si^{28} is very close to that observed with the natural Si samples, namely, 19% as compared to 18%.

The data reveals consistent differences (~55%) in the thermal conductivity between natural and isotopically-pure Si, independently of the level of Boron doping. The 55% gain is close to the 60% gain at room temperature reported by Capinski et al. [2] for intrinsically doped Si. From the current work, it can also be seen that the effects of isotopic purity and doping level are independent of each other. The loss in thermal conductivity of around 19% due to higher doping is smaller than that reported in reference [8] (~34%); however, the qualitative behavior of the results obtained in this work is consistent. A possible explanation for this discrepancy is the dependence of the specific heat (ρC_p) on the doping level. Since the numerical technique used to deduce the thermal conductivity requires (ρC_p) as an input parameter, uncertainties in the specific heat can result in errors in the calculated thermal conductivity. Unfortunately, the dependence of ρC_p on doping level and isotopic purity has not yet received attention in the open literature and remains an undeveloped issue.

The thermal interface resistance between the top gold layer and the underlying epitaxial layer appears to vary slightly from sample to sample. The range of the measured values falls within the envelope of the resistance reported by Käding et al. [9], namely, 0.8×10^{-8} to 4.3×10^{-8} m^2-K/W, indicating that the adhesion of the gold layer to the epitaxial material is very good. The interface between the epitaxially grown layer and the underlying Si wafer plays no role in the analysis since the epitaxial layer is thicker than the heat penetration depth during a complete measurement cycle. In other words, the ~500 ns duration of the cycle is not long enough for the heat front to interact with the interface between the epitaxial layer and the underlying Si wafer.

4. Conclusions

This paper reports on experiments conducted by a transient thermoreflectance technique (a) to measure the thermal conductivity and interface resistance of natural and isotopically-pure silicon and (b) to assess the effects of doping levels on the thermal conductivity. Since very few data exist for the thermal conductivity of isotopically-pure silicon, this work provides useful confirmation that isotopical purity increases thermal performance. The results obtained in this work are in good agreement with the previous results of Capinski et al. [3], and provide additional evidence to support the benefits of the use of Si^{28} (a gain of approximately 55% as compared to the thermal conductivity of natural silicon). Additionally, this

work has provided new data to assess the effects of Boron doping on the thermal conductivity as well as measurements of the specific values of the interface resistance that exist between the gold cover layer and the underlying epitaxial layer. Finally, since it was found that the effects of doping are the same for natural and isotopically-pure Si (a loss of approximately 19%), this work provides initial evidence to support the use for Si^{28} the available data that pertains to the influence of different levels of doping on the thermal conductivity of natural silicon.

Acknowledgements

The authors gratefully acknowledge Isonics Corp. of Golden, CO, for providing the research support to conduct this investigation. The authors are also thankful to Dr. Stephen Burden of Isonics who monitored the project and provided the required samples. The samples were covered with gold by Dr. Howard Beratan and his Raytheon colleagues at the uncooled detector branch of Raytheon in Dallas, TX. The authors are grateful to Dr. Beratan and Raytheon for providing this support at no cost to this project.

References

[1] The National Technological Roadmap for Semiconductors, International Sematech Corporation, http://www.sematech.org/public/publications/index.htm and http://public.itrs.net/files/1999_SIA_Roadmap/Home.htm

[2] W. S. Capinski, H. J. Maris, E. Bauser, I. Silier, M. Asen-Palmer, T. Ruf, M. Cardona, and E. Gmelin, "Thermal conductivity of isotopically enriched Si," *Appl. Phys. Lett*ers, Vol. 71, p. 2109, (1997)

[3] T. Ruf, R. W. Henn, M. Asen-Palmer, E. Gmelin, M. Cardona, H.-J. Pohl, G. G. Devyatych, and P. G. Sennikov, "Thermal conductivity of isotopically enriched Silicon," *Solid State Communications*, May (2000)

[4] D. Y. Tzou, *Macro to Microscale Heat Transfer (The Lagging Behavior)*, Taylor and Francis, Washington, DC Chapter 1, (1997)

[5] X. Xu, C. P. Grigoropoulos, and R. E. Russo, "Transient temperature during pulsed excimer laser heating of thin polysilicon films obtained by optical reflectivity measurement," *ASME Journal of Heat Transfer*, Vol. 117, pp. 17-24, (1995)

[6] I. Hatta, "Thermal diffusivity measurements of thin films and multilayered composites," *International Journal of Thermophysics*, Vol. 11, pp. 293-303, (1990)

[7] M. G. Burzo, P. L. Komarov, and P.E. Raad, "Influence of metallic absorption layer on the quality of thermal conductivity measurements by the transient thermo-reflectance method," *7th International Workshop on Thermal Investigations of ICs and Systems*, Paris, France, Sep. (2001)

[8] M. Asheghi, K. Kurabayashi, K. E. Goodson, R. Kasnavi, and J.D. Plummer, "Thermal Conduction in Doped Silicon Layers," submitted to the *33rd ASME/AIChE National Heat Transfer Conference*, Albuquerque, NM, August 8-14, (1999)

[9] O. W. Käding, H. Skurk, and K. E. Goodson, "Thermal conduction in metallized silicon-dioxide layers on silicon," *Appl. Phys. Lett*ers, Vol. 65, p. 1629, (1994)